Anatomy-Guided Discovery of Large-Scale Consistent Connectivity-Based Cortical Landmarks

Xi Jiang[1,*], Tuo Zhang[2,1,*], Dajiang Zhu[1], Kaiming Li[3], Jinglei Lv[2,1], Lei Guo[2], and Tianming Liu[1]

[1] Cortical Architecture Imaging and Discovery Lab, Department of Computer Science and Bioimaging Research Center, The University of Georgia, Athens, GA, USA
[2] School of Automation, Northwestern Polytechnical University, Xi'an, China
[3] Biomedical Imaging Technology Center, Emory University/Georgia Institute of Technology, Atlanta, GA, USA

Abstract. Establishment of structural and functional correspondences across different brains is one of the most fundamental issues in the human brain mapping field. Recently, several multimodal DTI/fMRI studies have demonstrated that consistent white matter fiber connection patterns can predict brain function and represent common brain architectures across individuals and populations, and along this direction, several approaches have been proposed to discover large-scale cortical landmarks with common structural connection profiles. However, an important limitation of previous approaches is that the rich anatomical information such as gyral/sulcal folding patterns has not been incorporated into the landmark discovery procedure yet. In this paper, we present a novel anatomy-guided discovery framework that defines and optimizes a dense map of cortical landmarks that possess group-wise consistent anatomical and fiber connectional profiles. This framework effectively integrates reliable and rich anatomical, morphological, and fiber connectional information for landmark initialization, optimization and prediction, which are formulated and solved as an energy minimization problem. Validation results based on fMRI data demonstrate that the identified 555 cortical landmarks are producible, predictable and exhibit accurate structural and functional correspondences across individuals and populations, offering a universal and individualized brain reference system for neuroimaging research.

Keywords: DTI, fMRI, anatomical, connectivity, cortical landmarks.

1 Introduction

Establishment of structural and functional correspondences across different brains is one of the most fundamentally important issues in the brain imaging field. Current popular approaches to establishing the correspondences of brains regions across individuals can be broadly classified into three categories: image registration algorithms [1-3], cortical parcellation [4, 5], and manual/semi-automatic regions of interests

[*] These authors contributed equally to this work.

K. Mori et al. (Eds.): MICCAI 2013, Part III, LNCS 8151, pp. 617–625, 2013.

(ROI) analysis [6, 7]. Although these methods have their own advantages and have been successfully applied in different scenarios [1-7], they are limited due to the lack of quantitative representation of the regularity and variability of brain structure and function. In recognition of this limitation, recent literature studies have proposed to automatically define and discover common and consistent brain ROIs/landmarks with intrinsic structural/functional correspondences in a group of subjects or populations [8-11]. The underlying neuroscience basis is that consistent white matter fiber connection patterns can be used as common landmarks to predict brain function [8-12]. However, those approaches [8-11] also have limitations in that they do not consider rich and meaningful anatomic information of human brains and the accuracy of the discovered brain landmarks can be significantly improved.

In response to the above challenges, in this paper, we propose a novel framework for large-scale consistent connectivity-based cortical landmark discovery that defines and optimizes landmarks via integrating reliable and rich anatomical, morphological, and connectional information. These meaningful constraints have been used for landmark initialization, optimization and prediction based on multimodal DTI/fMRI datasets. The major novelty of our framework is that based on the predefined gyral/sulcal folding pattern homology, our landmark optimization and prediction simultaneously consider structural connection pattern similarity and homogeneity, and landmark spatial constraint, all of which are computationally formulated into a unified energy minimization problem. The proposed framework discovers 555 cortical landmarks that are consistent, reproducible, and predictable across individuals and populations, as demonstrated by extensive validations. Our results suggest that this set of 555 cortical landmarks effectively represents common cortical architectures and potentially provides opportunities for numerous applications in brain sciences.

2 Materials and Methods

2.1 Overview

The framework includes three major steps as shown in the red boxes in Fig.1. We perform landmark initialization and optimization under the guidance of four constraints (green boxes) for model brains, and conduct landmark prediction for testing brains. Details will be presented in the following sections.

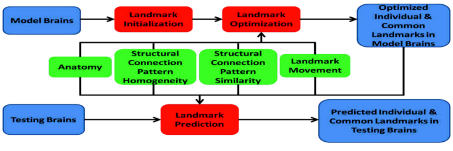

Fig. 1. The flowchart of the discovery of large-scale consistent cortical landmarks

2.2 Multimodal Data Acquisition, Preprocessing and Landmark Initialization

Two multimodal DTI/fMRI datasets were acquired and used in this work. In brief, dataset 1 includes DTI and four task-based fMRI scans (semantic decision making, emotion, empathy and fear networks) of eleven healthy young adults. Dataset 2

includes DTI and working memory task-based fMRI scans of twenty three healthy adult students. Imaging parameters and preprocessing steps of these datasets are referred to [10]. We randomly selected ten subjects from dataset 2 as the model brains. The other brains in datasets 1 and 2 were used as testing brains.

The landmark initialization procedure is as follows. First, we randomly selected one of the ten model brains as the template and other model brains were linearly registered to it via FSL FLIRT so that their global shape differences are removed and their cortical surfaces are in the same space for comparison. Second, for each corresponding major clearly identifiable gyrus/sulcus of each model brain according to the brain template used in the BrainVoyager Brain Tutor (http://www.brainvoyager.com), a certain number (ranging from 3-20) of landmarks were interactively labeled at cortical surface mesh vertices that are roughly distributed evenly along the gyral ridge/sulcal valley, and are sufficiently dense to ensure the full coverage of the whole gyral ridge/sulcal valley. In total, we manually labeled 594 landmarks for each model brain. It should be noted that during the following optimization step, the neighboring initialized landmarks that satisfy specific criteria are merged (Section 2.4). In this way, the number of initial landmarks (594) is not a critical issue. Since the variability of folding pattern across subjects is huge, the manually initialization and homology determination of the 594 roughly corresponding cortical landmarks in the ten model brains based on the gyral/sulcal folding patterns effectively enforces the first anatomy constraint for landmark optimization. That is, corresponding cortical landmarks in different brains should be located on the same clearly identifiable gyrus or sulcus in order to preserve the same anatomical identity.

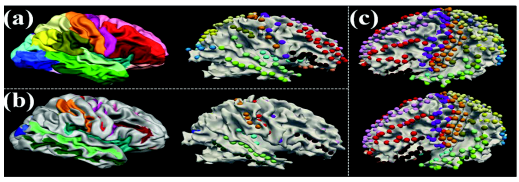

Fig. 2. The 594 manually labeled landmarks on the model brains. (a)-(b) show landmarks on the gyri/sulci of one model brain's right hemisphere, respectively. The landmarks and corresponding gyrus/sulcus are highlighted in the same color. (c) shows the 594 landmarks on two example model brains.

2.3 Structural Connection Pattern Similarity and Homogeneity Constraints

The second constraint for landmark optimization is that corresponding landmarks across ten model brains should possess similar structural connection patterns, which is represented by the DTI-derived fiber bundles emanating from the landmark. For each initialized landmark with extracted fiber bundles emanating around its neighbourhood, we used the trace-map model in [8], which is represented as a 144-dimenional vector, to quantitatively describe the structural connection pattern. Thus, the problem of quantitatively comparing the similarities across connections is converted to comparing the similarities across 144-dimenional trace-map vectors.

The third constraint for landmark optimization is that the corresponding landmarks across ten model brains should move toward to the location with local maximum of

structural connection pattern homogeneity, which is not considered in previous works [8-11]. The homogeneity is defined as the similarity between the trace-map representations of fiber bundles connected to the current ROI and its outside neighbouring ROIs, and calculated by the Kendall's coefficient of concordance [13]. Prior studies have demonstrated that the structural connection profile of a cortical ROI can be highly nonlinear, that is, a slight change to the location, size or shape to the ROI could significantly alters its fiber connection patterns [8, 11]. Therefore, this high nonlinearity can cause uncertainties and instabilities in the optimization and discovery of consistent and reproducible cortical landmarks. In this paper, we examined the nonlinearity of the entire cortex of the ten model brains, and found that there are cortical areas with substantially less nonlinearity, or more homogeneity. By measuring the fiber pattern similarity via the trace-map model as mentioned above, we found that the fiber patterns extracted from the local maximum of homogeneity (red bubbles) across corresponding landmarks in ten model brains have higher similarity than those extracted from the vertices in outside neighbourhoods, such as those in the 1-ring, 3-ring, and 5-ring surface mesh neighbourhood (yellow, green and purple bubbles). Fig. 3 suggests that there are cortical regions with homogeneity peaks on the cortex, and importantly, these peaks exhibit quite consistent fiber connection patterns. Thus, the initialized landmarks across ten model brains should move toward to the cortical regions with homogeneity peaks within a neighborhood. The fourth constraint for landmark optimization is that the landmark should move within a neighborhood of the initial location with a predefined size.

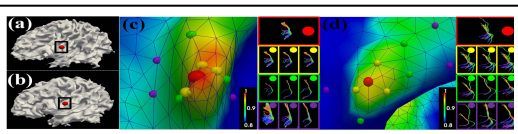

Fig. 3. Structural connection pattern homogeneity. (a)-(b): one corresponding landmark in two model brains. (c)-(d): Cortical regions are plotted by homogeneity values. The color bar is in the bottom right. Local maximum of homogeneity and example vertices in its 1-ring, 3-ring and 5-ring neighborhood are shown in red, yellow, green and purple bubbles, respectively. The fiber shape patterns of the colored bubbles in the left panel are shown in the right panel.

2.4 Landmark Optimization

With the availability of initialized cortical landmarks in Section 2.2 and four meaningful constraints in Sections 2.2-2.3, we performed landmark optimization by searching all possible combinations of candidate landmark locations within their local morphological neighbourhoods in different model brains, and to seek the optimal solution with the optimal group-wise consistency and homogeneity. In this paper, we formulated and solved the landmark optimization problem by jointly modeling the four constraints. The goal is to minimize the group-wise variance of these jointly modeled profiles. Assume that there are M brains (i is i-th brain) and j is the current landmark that to be optimized. $\tilde{k}_i^j$ is the initial location of j in brain i, and k_i^j is the candidate location in its neighborhood $C_{\tilde{k}_i^j}$ ($k_i^j \in C_{\tilde{k}_i^j}$). The maximum principal

curvature of k_i^j is represented by $p_{k_i^j}\begin{cases}\geq 0, gyrus\\ < 0, sulcus\end{cases}$ and it is used as the anatomical constraint in the following energy function. Mathematically, the group-wise variance is modeled as the energy E that we want to minimize as follows.

$$E(j) = \lambda_1 E_S(j) + \lambda_2 E_H(j) + \lambda_3 E_D(j), \quad k_i^j \in \mathrm{C}_{\tilde{k}_i^j} \text{ and } p_{k_i^j}\begin{cases}\geq 0, gyrus\\ < 0, sulcus\end{cases} \tag{1}$$

where E_S is the structural connection pattern similarity constraint, E_H is the structural connection pattern homogeneity constraint, and E_D is the landmark movement constraint. Here, we have weights $\lambda_1 + \lambda_2 + \lambda_3 = 1$ $(0 \leq \lambda_1, \lambda_2, \lambda_3 \leq 1)$.

First, $E_S(j)$ is defined to ensure that the corresponding landmark j across M brains have similar fiber bundle shape patterns as mentioned in Section 2.3.

$$E_S(j) = var\left(\left\{tr\left(k_1^j\right), tr\left(k_2^j\right), \ldots, tr\left(k_i^j\right)\right\}\right) \tag{2}$$

where $tr(k_i^j)$ is a 144-dimension trace-map vector of k_i^j. var(·) is the variance.

Second, $E_H(j)$ is defined to ensure that the corresponding landmark j across M brains should move toward to the location with local maximum of homogeneity within $\mathrm{C}_{\tilde{k}_i^j}$. We assume there are Q vertices in the candidate vertex's neighborhood $\mathrm{C}_{\tilde{k}_i^j}$ and they are regarded as the objects to be ranked. Each of 144 dimensions of trace-map is considered as a judge [13] and the number of judges is denoted by P. Define object q is given the rank $r_{q,p}$ by judge p, t_k is the number of tied ranks in k-th of m groups of ties. The Kendall's coefficient of concordance [13] of landmark j of brain i is defined as

$$W_i^j\left(tr(k_i^j)\right) = \frac{12\sum_{q=1}^{Q}\left(\sum_{p=1}^{P} r_{q,p}\right)^2 - 3P^2Q(Q+1)^2}{P^2(Q^3-Q) - P\sum_{k=1}^{m}(t_k^3 - t_k)} \tag{3}$$

$$E_H(j) = \sum_{i=1}^{M}\left(1 - W_i^j\left(tr(k_i^j)\right)\right) \tag{4}$$

Third, $E_D(j)$ is defined to ensure the landmark j moves within $\mathrm{C}_{\tilde{k}_i^j}$ where $p_{k_i^j}\begin{cases}\geq 0, gyrus\\ < 0, sulcus\end{cases}$ during the optimization procedure.

$$E_D(j) = \sum_{i=1}^{M} dist\left(k_i^j, \tilde{k}_i^j\right) \tag{5}$$

where $dist(\cdot)$ is the Euclidean distance between k_i^j *and* $\tilde{k}_i^j$ on the cortical surface.

The energy minimization is solved as follows. For each iteration, by searching the whole-space of landmarks candidate locations in different model brains for one corresponding landmark, we can find an optimal combination of landmark locations that minimizes E (Eq. (1)). The convergence criterion is that the distance of landmark locations between two consecutive iterations is less than ε (ε = 2 mm, since the distance between two adjacent surface mesh vertices is about 2 mm). Notably, for each

iteration, if the distance between two neighboring landmarks to be optimized is less than or equal to a threshold t_d (t_d =2 mm, since the distance between two adjacent surface mesh vertices is about 2 mm) across $p\%$ (here p=80) of all model subjects, we label these two landmarks as 'merged' and only optimize one of them in the next iteration. In our implementation, we considered about 30 candidate locations (3-ring neighborhood) for each landmark. We tested different combinations of λ_1, λ_2 and λ_3 in Eq. (1) and chose the ones with best optimization results (for gyri, $\lambda_1 = 0.5, \lambda_2 = 0.4$ and $\lambda_3 = 0.1$ and for sulci, $\lambda_1 = 0.6, \lambda_2 = 0.3$ and $\lambda_3 = 0.1$). Other efficient approaches for energy minimization may be considered in the future.

2.5 Landmark Determination and Prediction

To examine and ensure the reproducibility of the discovered cortical landmarks, we divided the ten model brains into two groups and performed landmark optimization separately. As a result, two independent groups of optimized cortical landmarks were obtained. Then, for each optimized landmark in all of the ten brains in two groups, we evaluated the consistency of landmarks using both quantitative (trace-map similarity [8]) and qualitative (visual inspection) methods the same as in [10]. In brief, for each corresponding landmark, we calculated its mean trace-map distance [8], which measures the similarity of fiber shape patterns, between two groups and adopted the same criterion in [10] to verify if the landmark was similar across groups of brains [8, 10]. Furthermore, we used in-house batch visualization tool [10] to visually check the fiber patterns in all model brains of two groups. If the landmark in any of the ten model brains has substantially different trace-map distance value, and is confirmed to have different fiber shape patterns by visual inspection, this landmark is discarded. Finally, we retained 555 landmarks which exhibit consistent fiber connection patterns across all ten model brains.

Based on the 555 landmarks in the ten model brains, we predicted them in other testing brains (Section 2.2). Given a testing brain, we first mapped the 555 landmarks of one model brain to the testing brain via linear image registration (FSL FLIRT) to have rough locations. Then we optimized the locations of the 555 landmarks on the testing brain by minimizing the energy E (Eq. (1)) across ten model brains and the testing brain. The landmark prediction procedure is fast and efficient (about 15 minutes for one testing brain on a typical PC).

3 Experimental Results

3.1 Reproducibility and Predictability of 555 Cortical Landmarks

Figs. 4a-4b show the 555 landmarks (yellow bubbles) in three model brains and three testing brains, respectively. As an example, we randomly selected 5 landmarks and visualized their fiber connectional patterns in the three model and three testing brains in the left and right panel of Fig. 4, respectively. Quantitatively, the average trace-map distances of the corresponding landmarks across model and testing brains are 2.08, 2.18, 2.15, 2.20 and 2.24, respectively, which are considered as quite low [8, 10]. By visual inspection, there is also no much difference among the fiber patterns of

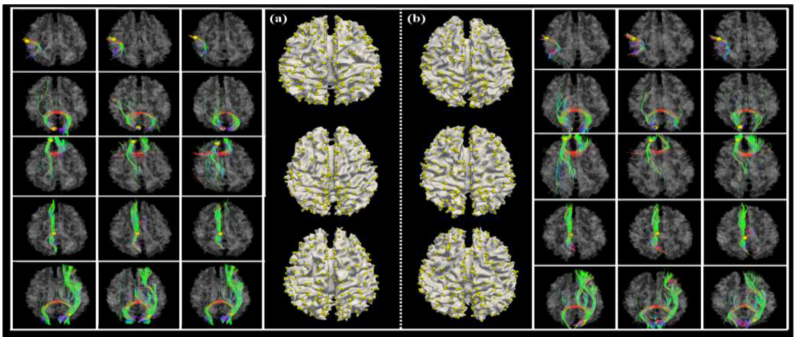

Fig. 4. The 555 landmarks (yellow bubbles) in (a) three model brains and (b) three testing brains, respectively. Five landmarks are randomly selected and their fiber connectional patterns in the model and testing brains are shown in the left and right panel, respectively.

the same corresponding landmark in all model and testing brains. Importantly, all of these 555 landmarks have been confirmed to possess the above-mentioned characteristics in all ten model brains and testing brains, indicating that the 555 landmarks represent a common structural brain architecture that is reproducible and predicable across different subjects.

3.2 Functional Annotation of Landmarks

We adopted the two fMRI datasets including five task-based scans in Section 2.2 to examine the functional roles and correspondences of the 555 DTI-derived cortical landmarks. The benchmark fMRI activation peaks were detected and selected using FSL FEAT as the functional locations. In total, we identified 69 functional locations from the five functional networks. For each functional location, we first identified five closest (Euclidean distance) cortical landmarks within each model brain as the candidates. Then, the cortical landmark with the most votes as the closest to the functional location across all ten model brains was annotated by the functional location. In total, 46 cortical landmarks were annotated. The same cortical landmark is truly in the specific functional network across all subjects,

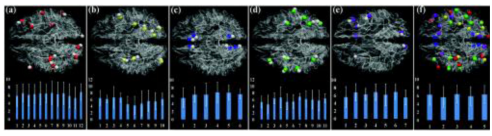

Fig. 5. Functional annotation of the cortical landmarks by fMRI-derived functional locations in five networks shown on one model brain. (a) semantic decision making; (b) emotion; (c) empathy; (d) fear; (e) working memory; In each sub figure, the functional locations are highlighted by white bubbles and the annotated landmarks are highlighted by other color bubbles. The mean distance and standard deviation between each pair of functional location and landmark are shown in the histogram. (f) all functionally annotated landmarks. The mean distance and standard deviation between each pair of functional location and landmark within each of five networks are illustrated in the histogram.

suggesting that these landmarks specifically align with regions of task-related processing. The mean distances for the five functional networks are 6.27 mm 5.68 mm, 6.38 mm, 5.91 mm and 6.33 mm, respectively. On average, the distance is 6.11 mm. The results in Fig. 5 demonstrate the corresponding structural connectivity-based landmarks are consistently co-localized with the same functional regions, and reflect the common structural/functional cortical architectures that are reproducible across subjects. It should be noted that more cortical landmarks may be functionally annotated if more specific, large-scale fMRI tasks can be designed and performed in the future for the purpose of functional annotation of landmarks.

3.3 Comparisons with Image Registration Algorithms

Finally, we compared the functional annotation accuracies by our 555 landmarks and those by four different linear/nonlinear image registration algorithms (linear: FSL FLIRT; nonlinear: FSL FNIRT, ANTS, and HAMMER). The working memory functional locations in Fig. 5 were used as benchmarks. The average annotation errors by the five methods (our landmarks, FSL FLIRT, FSL FNIRT, ANTS and HAMMER) are 6.33 mm, 7.76 mm, 8.01 mm, 7.74 mm, and 7.73 mm respectively, indicating that our landmarks have superior functional annotation accuracy than those four image registration algorithms.

4 Conclusion

In this paper, we presented a novel anatomy-guided discovery framework to define and optimize a dense map of cortical landmarks that possess group-wise consistent anatomical/connectional profiles. Extensive experiments demonstrated its reproducibility and predictability. Furthermore, a validation study via task-based fMRI was provided for a subset of the discovered landmarks, suggesting the accurate structural and functional correspondences of these landmarks across individuals and populations. In the future, we will compare our 555 landmarks with the available DICCCOL system [10]. Other possible future studies will apply this dense map of 555 landmarks as a universal and individualized brain reference system on clinical datasets for connectivity analysis and mapping human brain connectomes.

References

1. Thompson, P., Toga, A.W.: A surface-based technique for 1336 warping 3-dimensional images of the brain. IEEE Trans. Med. Imaging 15(4), 402–417 (1996)
2. Fischl, B., et al.: Whole brain segmentation: automated labeling of neuroanatomical structures in the human brain. Neuron 33(3), 341–355 (2002)
3. Shen, D., Davatzikos, C.: HAMMER: hierarchical attribute matching mechanism for elastic registration. IEEE Trans. Med. Imaging 21(11), 1421–1439 (2002)
4. Johansen-Berg, et al.: Changes in connectivity profiles define functionally distinct regions in human medial frontal cortex. Proceedings of the National Academy of Sciences of the United States of America (PNAS) 101(36), 13335–13340 (2004)

5. Jbabdi, S., et al.: Multiple-subjects connectivity-based parcellation using hierarchical Dirichlet process mixture models. NeuroImage 44(2), 373–384 (2009)
6. Poldrack, R.A.: The future of fMRI in cognitive neuroscience. NeuroImage (2011), doi:10.1016/j.neuroimage.2011.08.007
7. Liu, T.: A few thoughts on brain ROIs. Brain Imaging and Behavior (2011), doi:10.1007/s11682-011-9123-6
8. Zhu, D., et al.: Discovering Dense and Consistent Landmarks in the Brain. In: Székely, G., Hahn, H.K. (eds.) IPMI 2011. LNCS, vol. 6801, pp. 97–110. Springer, Heidelberg (2011)
9. Zhang, T., et al.: Predicting functional cortical landmarks via DTI-derived fiber shape models. Cerebral Cortex (2011)
10. Zhu, D., et al.: DICCCOL: Dense Individualized and Common Connectivity-based Cortical Landmarks. Cerebral Cortex (2012), doi:10.1093/cercor/bhs072
11. Li, K., et al.: Individualized ROI Optimization via Maximization of Group-wise Consistency of Structural and Functional Profiles. In: Advances in Neural Information Processing Systems, NIPS (2010)
12. Honey, C.J., et al.: Predicting human resting-state functional connectivity from structural connectivity. Proceedings of the National Academy of Sciences of the United States of America (PNAS) 106(6), 2035–2040 (2009)
13. Siegel, S., Castellan Jr., N.J.: Nonparametric Statistics for the Behavioral Sciences, 2nd edn., p. 266. McGraw-Hill, New York (1988)